Supporting Information for

Trapping a crosslinked lysine–tryptophan radical in the catalytic cycle of the radical SAM enzyme SuiB

Aidin R. Balo[1], Alessio Caruso[2], Lizhi Tao[1], Dean J. Tantillo[1], Mohammad R. Seyedsayamdost[2,3]*, R. David Britt[1]*.

Affiliations:

[1]Department of Chemistry, University of California, Davis, CA, 95616, United States

[2]Department of Chemistry, Princeton University, Princeton, NJ, 08544, United States

[3]Department of Molecular Biology, Princeton University, Princeton, NJ, 08544, United States

*Correspondence to: mrseyed@princeton.edu, rdbritt@ucdavis.edu

This PDF file includes:

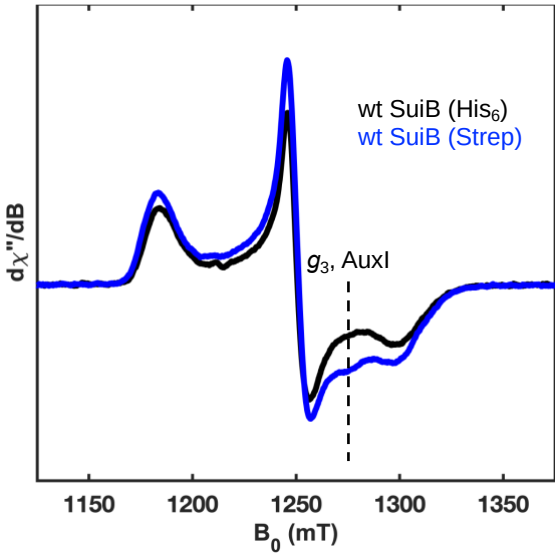

Fig. S1. Q-band EPR spectra of SuiB purified either using a His_6 tag followed by Fe-S reconstitution or using a Strep tag. The His_6-tagged protein is missing a significant fraction of its AuxI clusters relative to the Strep-tagged protein (dotted line). See Figure 3A for spectral assignments of clusters. The Lys–Trp• intermediate could not be observed using the His_6-tagged enzyme. Further, EPR spectra with a site-directed mutant that no longer binds AuxII (AuxII knockout mutant; AuxIIko) in Figure S4 suggest that the His_6 tag purification protocol also has an adverse effect on the RS cluster relative to the Strep tag purification protocol.

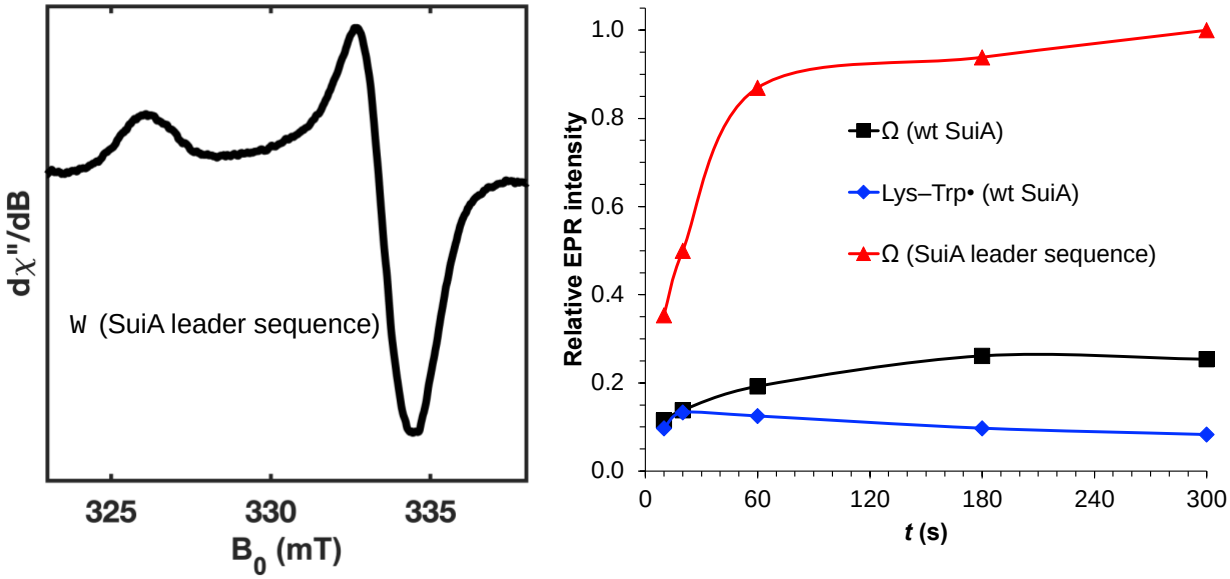

Fig. S2. (Left) The EPR spectrum of Ω generated through the leader sequence peptide, closely resembling spectrum 3 in Figure 2A. (Right) Relative concentrations of paramagnetic intermediates trapped by flash freezing enzymatic reaction samples at various times (*t*) using either the substrate (wt SuiA) or a substrate analogue containing only the SuiA leader sequence peptide, SuiA (-14)–(-1). In the reaction with wt SuiA, the concentration of Lys–Trp• exhibits an initial burst phase, reaching a maximum at ~20s and gradually decreasing as the reaction approaches steady state after ~1 min. Levels of Ω increase upon reaction initiation until steady sate (~1 min). In the reaction of SuiB with the SuiA leader peptide, Lys–Trp• is not observed, and Ω follows the same trend as in wt SuiA, but with a 4-fold increase in signal intensity.

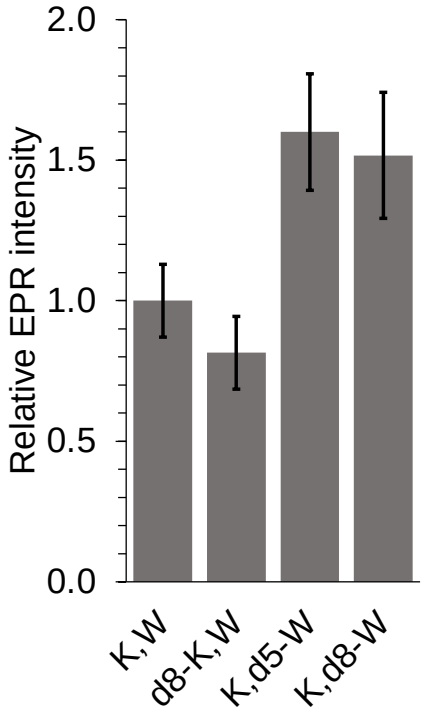

Fig. S3. The effect of selective deuteration on the relative concentration of Lys–Trp• observed after 20 s. Lys2 side chain deuteration decreases [Lys–Trp•] by ~20%. Conversely, Trp6 indole and uniform deuteration increase [Lys–Trp•] by ~60%. The error bars represent the standard deviation of samples prepared in triplicates.

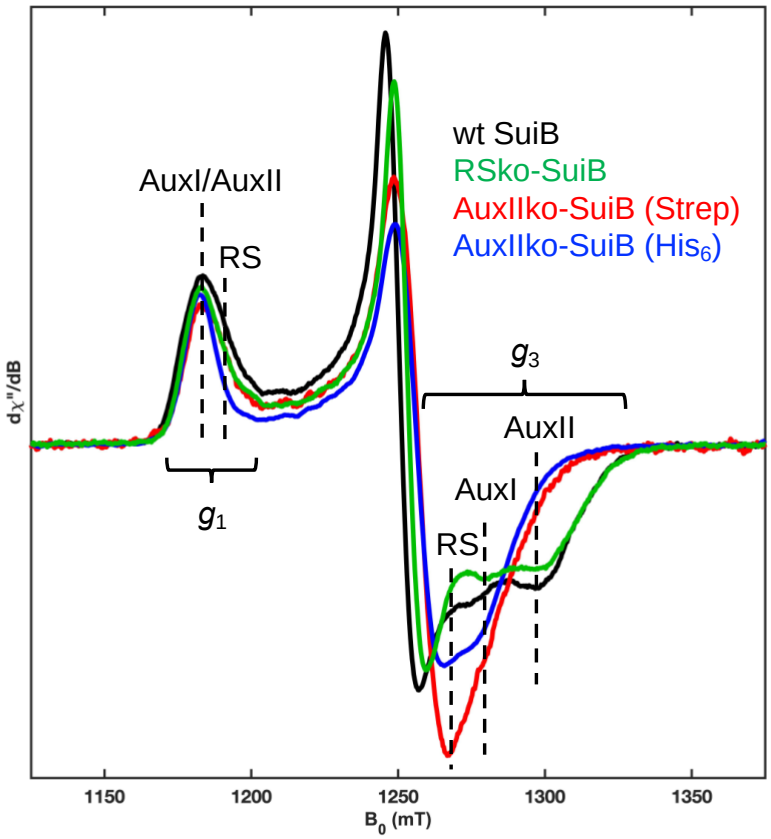

Fig. S4. EPR spectra used to deconvolute the signal of each Fe-S cluster in Figure 3A. The g_1 and g_3 components of each cluster are highlighted. The Strep–AuxII knockout mutant (C409A/C415A) allowed for straightforward deconvolution of the dominating AuxII cluster signal. The RS cluster knockout mutant (C121A/C124A) allowed for separation of the RS cluster signal. While an RS cluster signal could be obtained this way, it resulted in a poor S/N ratio due to the low signal intensity of the RS cluster in the wt SuiB (see Figure 3B). Varying the preparation of the AuxII knockout mutant (His_6 vs. Strep tag) resulted in great contrast between residual RS cluster and AuxI cluster spectral components, presumably due to an adverse effect that the His_6 preparation exhibits on the RS cluster. Consistent with prior studies (*1*), the AuxI knockout mutant (C321A/C365A) was not soluble and therefore could not be purified.

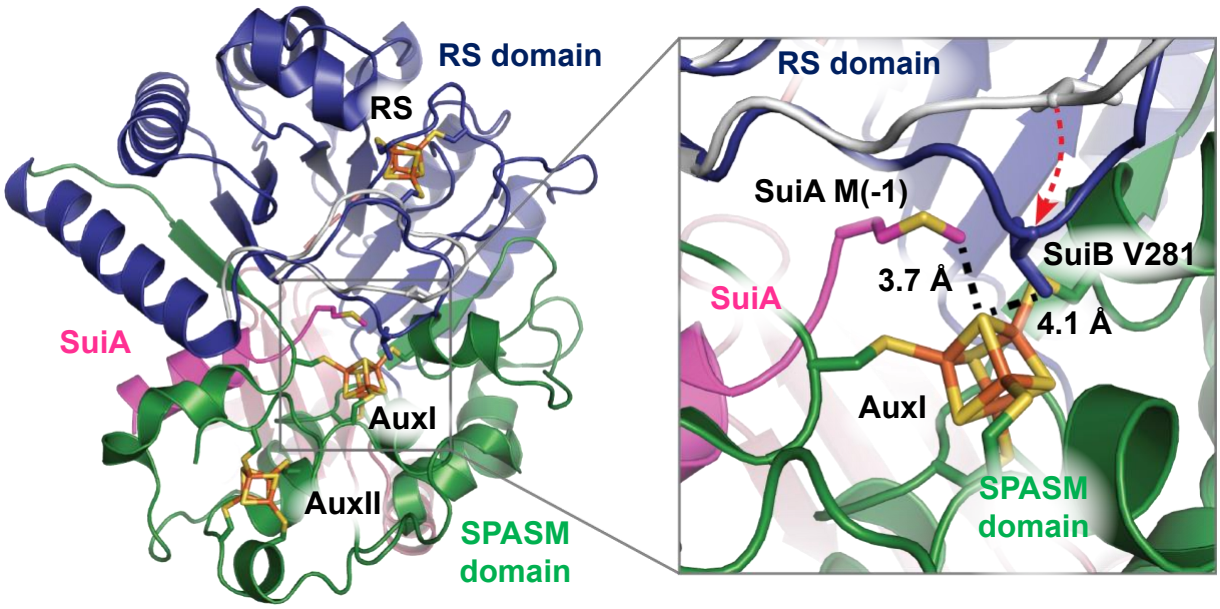

Fig. S5. Crystallographic comparison showing interaction between AuxI of SuiB and substrate SuiA (PDB ID: 5V1S, 5V1T) (*2*). Features of the apo-SuiA structure are shown in grey, while the SuiA-bound structure is colored by domain. Upon binding SuiA in both wt SuiB and RSko-SuiB, the EPR signal of AuxI diminishes (See Figure 3B). Only the leader sequence portion of SuiA is resolved in the crystal structure (residues -14 to -1).

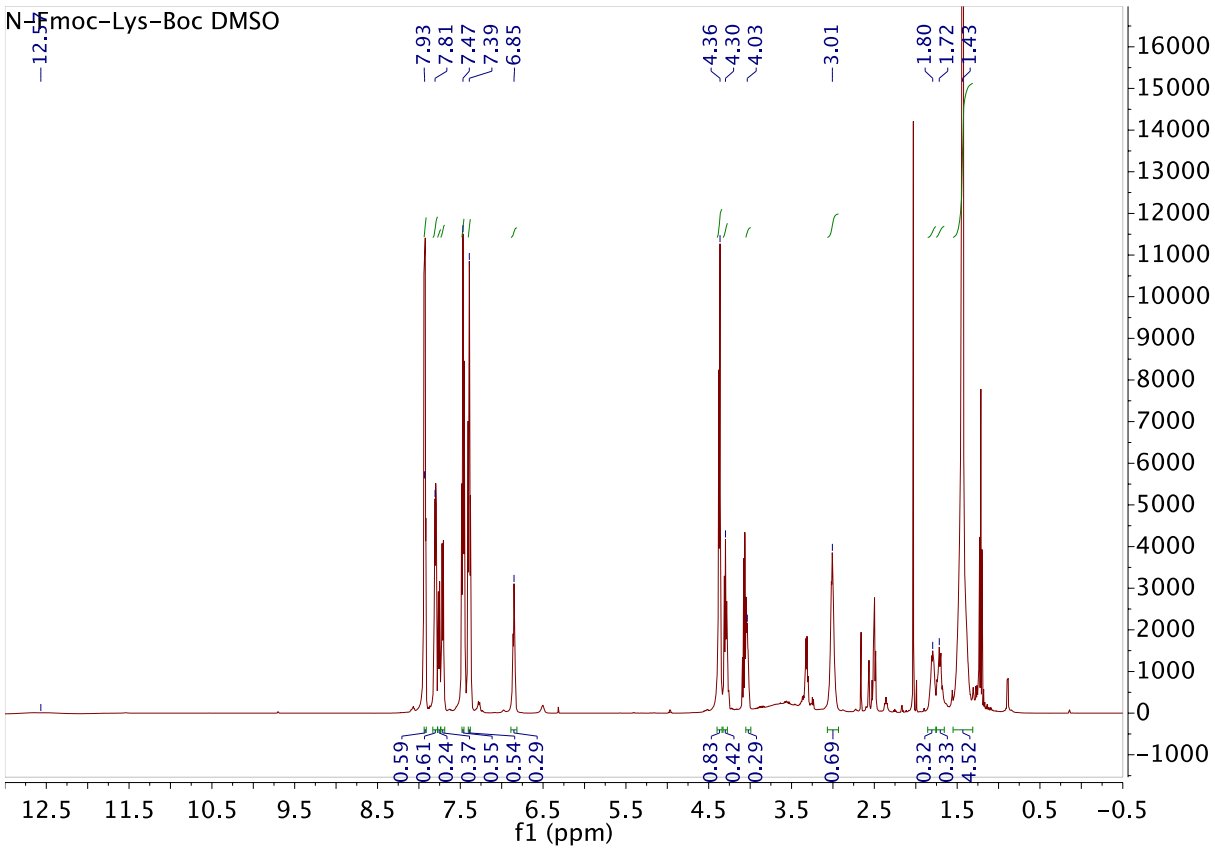

Fig. S6. ^{1}H-NMR spectrum of Fmoc-L-Lys(Boc)-OH used in SuiA synthesis.

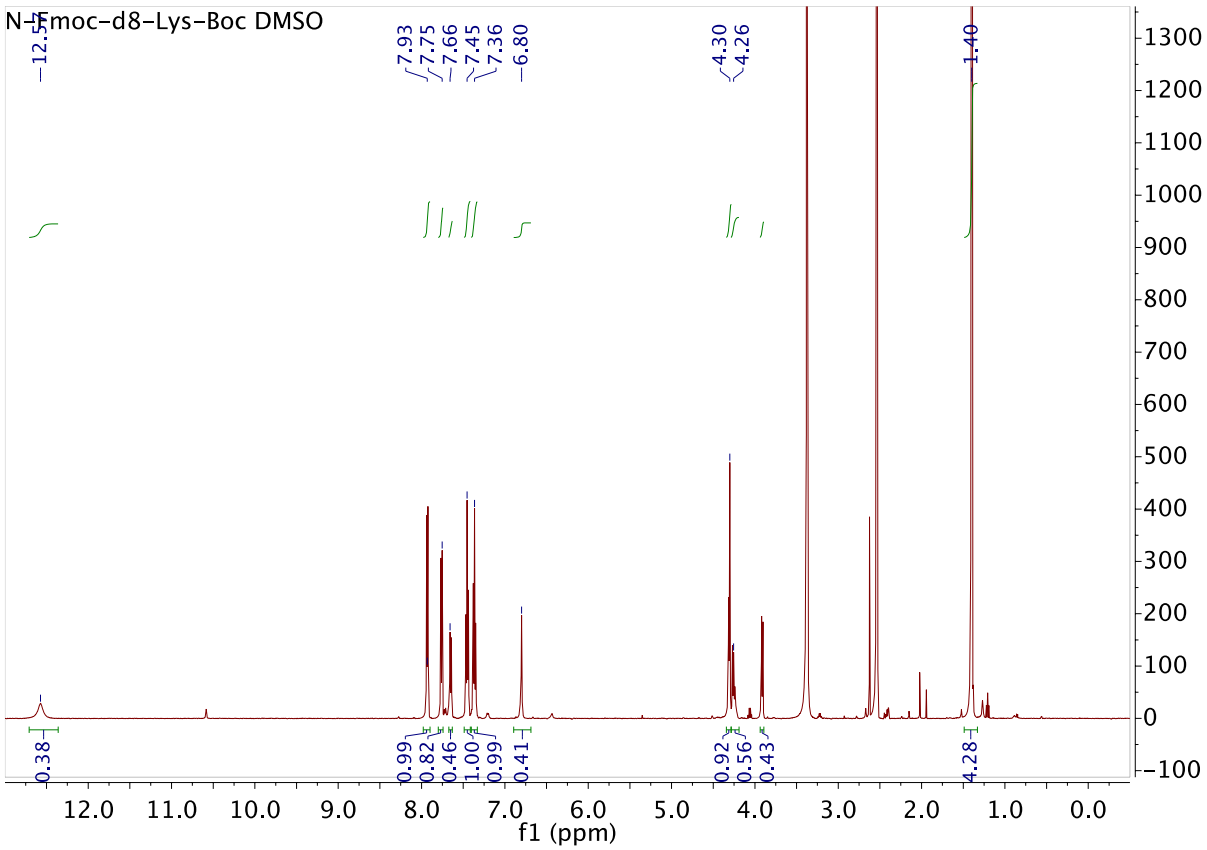

Fig. S7. ^{1}H-NMR spectrum of Fmoc-d_8-L-Lys(Boc)-OH used in SuiA synthesis.

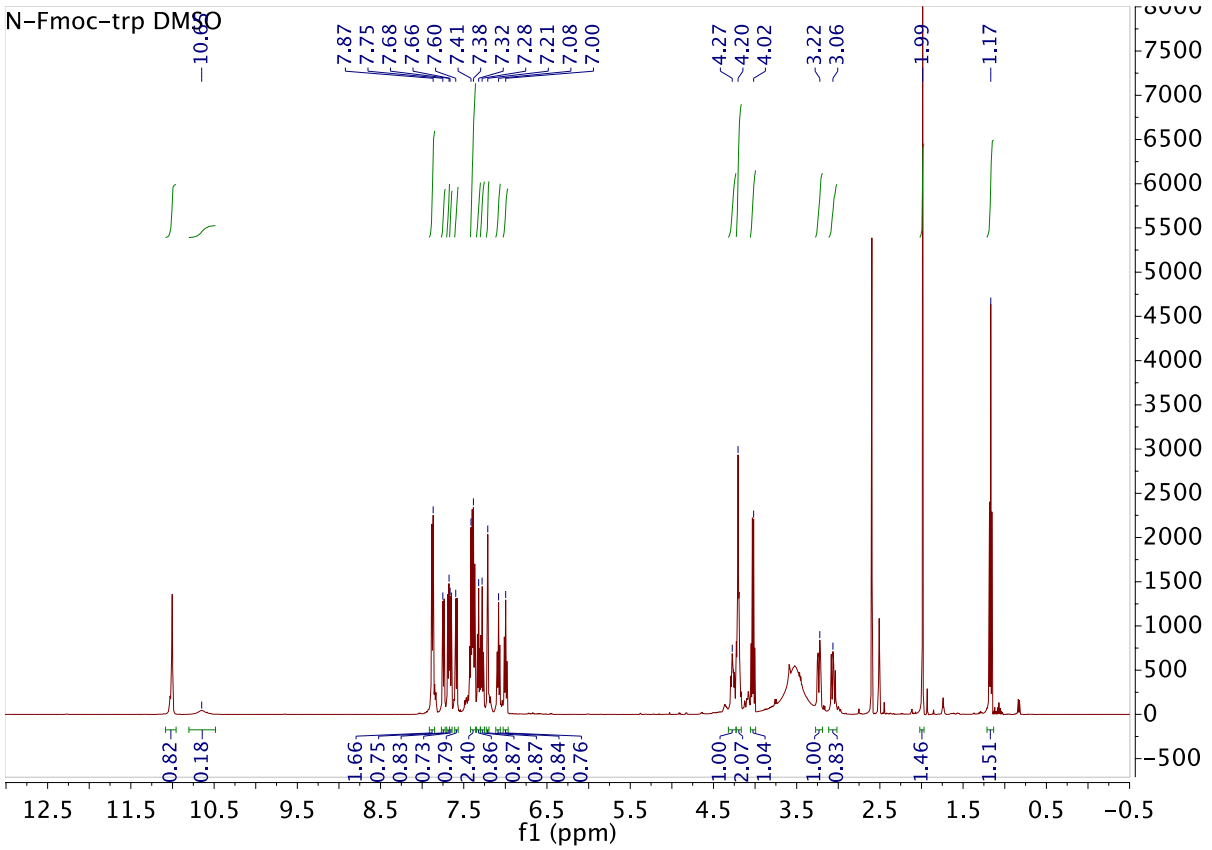

Fig. S8. ^{1}H-NMR spectrum of Fmoc-L-Trp-OH used in SuiA synthesis.

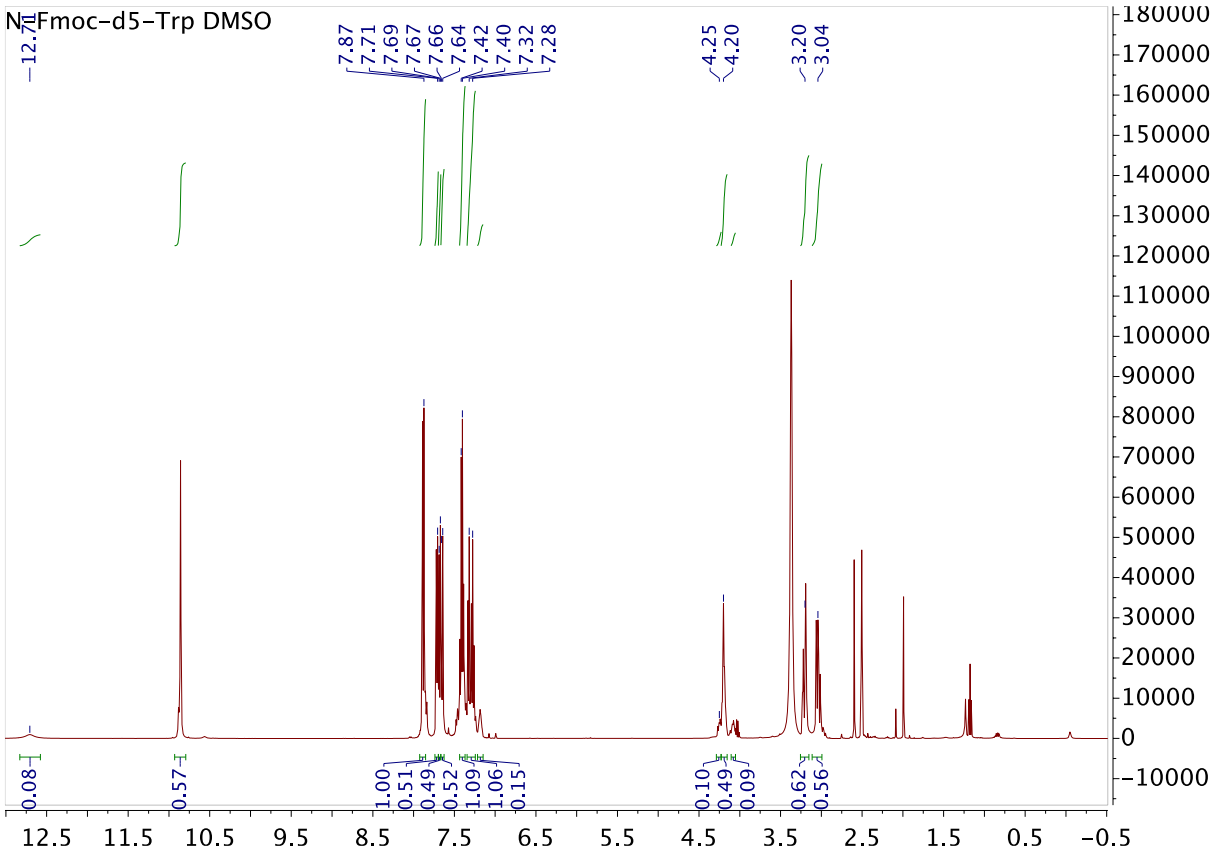

Fig. S9. ^{1}H-NMR spectrum of Fmoc-d_5-L-Trp-OH used in SuiA synthesis.

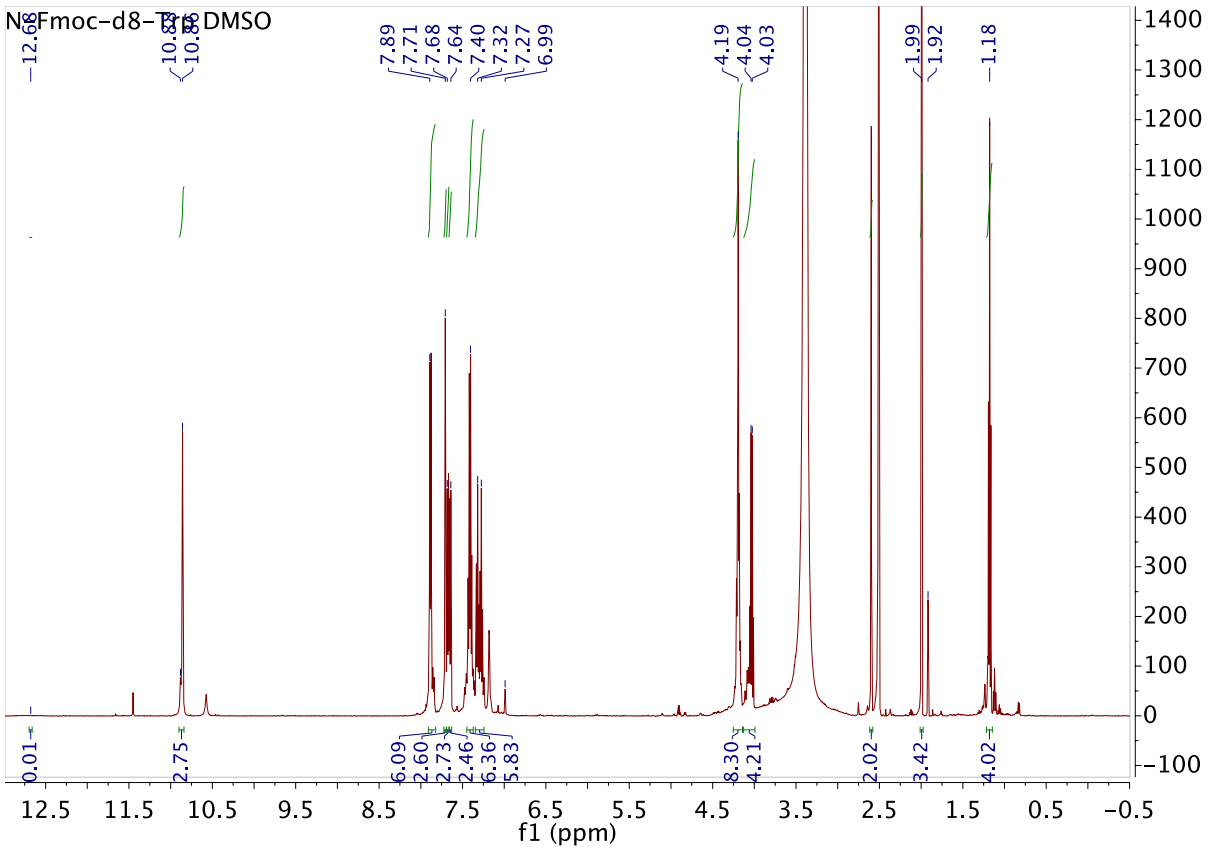

Fig. S10. ^{1}H-NMR spectrum of Fmoc-d_8-L-Trp-OH used in SuiA synthesis.

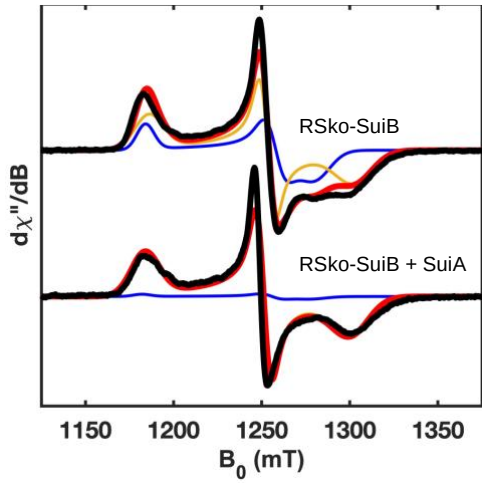

Fig. S11. The effect of obtaining a low-potential AuxI cluster upon binding SuiA shown in Figure 3B is also apparent in RSko-SuiB, in which the signal intensity of AuxI relative to AuxII decreases from 45% to 5%.

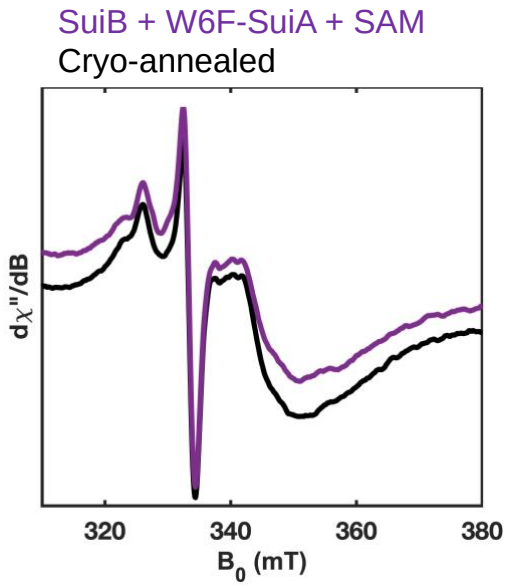

Fig. S12. Using a SuiB + DT + W6F-SuiA + SAM "reaction" sample as a negative control for the cryo-annealing result shown in Figure 3C. In the absence of the substrate Trp6, the clear accumulation of the modified AuxI signal upon cryo-annealing at 200 K for 10 min is not observed.

Table S1. Comparison of various tryptophan radicals to SuiA Lys–Trp•.

Species	*g*	$\lvert A_{N1}\rvert$ (mT)	$\lvert A_{H1}\rvert$ (mT)	$\lvert A_{H2}\rvert$ (mT)	$\lvert A_{H\beta1,W}\rvert$ (mT)	$\lvert A_{H\beta2,W}\rvert$ (mT)	$\lvert A_4\rvert$ (mT)	$\lvert A_5\rvert$ (mT)	$\lvert A_6\rvert$ (mT)	$\lvert A_7\rvert$ (mT)	$\lvert A_{H\beta,K}\rvert$ (mT)
EPR	2.0042						0.71		**1.78**	**2.85**	
K16–W20•	2.0042						**1.78**		0.71	**2.85**	
SuiA/SuiB	2.0042						**1.07**		**1.07**	**2.85**	
DFT	2.0022	0.08	0.02	0.05	0.05	0.21	0.56	0.51	**1.77**	**4.20**	0.00
K16–W20•	2.0026	0.07	0.15	0.04	0.02	0.11	**2.07**	0.25	0.46	**4.34**	0.23
SuiA/SuiB	2.0030	0.05	0.16	0.06	0.02	0.10	**1.35**	0.18	**1.18**	**4.12**	0.05
EPR (*3*)	2.0035		0.10	0.28	**2.35**	**1.13**	0.64				N/A
W•	2.0025		0.19	0.04	**2.75**	**1.13**			0.62		
P. eryngii VP	2.0022	**1.00**	0.07	0.11	**2.70**	**1.18**	0.49		0.46		
EPR (*4*)	2.0035				**2.15**	**1.75**	0.64				N/A
W•	2.0025				**2.30**	**1.95**			0.62		
B. adusta VP	2.0022	**1.05**			**2.30**	**1.95**	0.49		0.46		
EPR (*5*)	2.0033		0.11		**2.70**	**1.38**	0.68				N/A
W111• Y122F	2.0024		0.19		**2.75**	**1.38**			0.61		
E. coli RNR	2.0021	**1.05**	0.07		**2.83**	**1.38**	0.50		0.51		
EPR (*5*)	2.0035					**2.25**	0.56				N/A
W177• Y177F	2.0025					**2.25**			0.63		
E. coli RNR	2.0023	0.94				**2.25**	0.46		0.52		
EPR (*6*)	2.0036				0.75	0.58	0.60		0.53		N/A
W48•	2.0027				0.75	0.58					
AzC	2.0022	**1.07**			0.98	0.83	0.51		0.36		
EPR (*6*)	2.0035				0.16	**1.02**	0.77		0.64		N/A
W108•	2.0026				0.16	**1.39**					
ReAzs	2.0022	0.83			0.51	**1.39**	0.46		0.54		
DFT (*3*)	2.0037	0.13	0.08	0.16	**2.79**	**1.07**	0.60		0.10		N/A
W•	2.0029	0.12	0.18	0.07	**3.06**	**1.12**	0.18		0.56		
(21° from plane)	2.0025	**1.19**	0.06	0.15	**2.85**	**1.38**	0.48		0.37		

Table S2. Energy required for oxidation of radical anions to neutral molecules acquired experimentally as well as through DFT calculations at the M06-2X/6-31+G(d,p) level of Lys–Trp•⁻ and similar compounds.

Species	**Energy required for oxidation (experimental)** (*7*)	**Energy required for oxidation (computational)**
Lys–Trp•⁻ Doubly methyl-capped	N/A	-21 kcal/mol
Lys–Trp•⁻ Macrocyclic	N/A	-8 kcal/mol
Indole anion	+0.1 kcal/mol	0 kcal/mol
Benzaldehyde anion	+9 kcal/mol	+10 kcal/mol
Benzophenone anion	+15 kcal/mol	+16 kcal/mol
Nitrobenzene anion	+23 kcal/mol	+28 kcal/mol

Table S3. DFT atomic coordinates (in Å) used in Figure 2B.

C	1.104058	-3.888502	-0.058082
C	0.639267	-2.560566	0.462690
C	-0.149603	-2.322399	1.583589
C	0.927853	-1.262443	-0.113780
C	1.676119	-0.857898	-1.264236
C	0.293487	-0.289965	0.694672
N	-0.346856	-0.951662	1.710386
C	1.750822	0.531146	-1.556534
C	0.338273	1.193046	0.476502
C	1.135191	1.497542	-0.774857
H	0.736394	-4.721637	0.572966
H	2.213301	-3.953126	-0.088587
H	0.748763	-4.069486	-1.095567
H	-0.588851	-3.021095	2.304617
H	2.177402	-1.597962	-1.904934
H	-0.897780	-0.510367	2.447514
H	2.320504	0.855945	-2.442761
H	-0.707681	1.570557	0.326376
H	1.226918	2.561370	-1.047792
C	0.892830	1.962554	1.707188
H	0.903760	3.053711	1.509161
H	0.267246	1.788160	2.606778
H	1.928581	1.637077	1.931691

Table S4. Summary of $[4Fe\text{-}4S]^{+}$ *g*-tensors reported.

Cluster	Solution strategy	g_1	g_2	g_3
RS	Knockout mutation, 10K	2.048	1.936	1.916
AuxI	Knockout mutation, 10K	2.060	1.939	1.904
AuxII	Knockout mutation, 10K	2.057	1.946	1.872
AuxI	Reaction sample without SuiA, 35K	2.066	1.946	1.905
AuxI	Cryo-annealed reaction sample, 35K	2.075	1.944	1.908

Supporting Information References

1. K. R. Schramma, L. B. Bushin, M. R. Seyedsayamdost, Structure and biosynthesis of a macrocyclic peptide containing an unprecedented lysine-to-tryptophan crosslink. *Nat Chem* **7**, 431-437 (2015).
2. K. M. Davis *et al.*, Structures of the peptide-modifying radical SAM enzyme SuiB elucidate the basis of substrate recognition. *Proc Natl Acad Sci U S A* **114**, 10420-10425 (2017).
3. R. Pogni *et al.*, A tryptophan neutral radical in the oxidized state of versatile peroxidase from Pleurotus eryngii: a combined multifrequency EPR and density functional theory study. *J Biol Chem* **281**, 9517-9526 (2006).
4. R. Pogni *et al.*, Tryptophan-based radical in the catalytic mechanism of versatile peroxidase from Bjerkandera adusta. *Biochemistry* **44**, 4267-4274 (2005).
5. G. Bleifuss *et al.*, Tryptophan and tyrosine radicals in ribonucleotide reductase: a comparative high-field EPR study at 94 GHz. *Biochemistry* **40**, 15362-15368 (2001).
6. S. Stoll *et al.*, Hydrogen bonding of tryptophan radicals revealed by EPR at 700 GHz. *J Am Chem Soc* **133**, 18098-18101 (2011).
7. P. J. Linstrom, NIST chemistry webbook. *http://webbook.nist.gov*, (2005).